WADC TECHNICAL REPORT 59-416
PART IV

INVESTIGATION OF CREEP BUCKLING OF COLUMNS AND PLATES

PART IV. COLUMN CREEP BUCKLING THEORY AND CORRELATION WITH EXPERIMENTS

GEORGE GERARD
RALPH PAPIRNO

NEW YORK UNIVERSITY

JULY 1961

DIRECTORATE OF MATERIALS AND PROCESSES
CONTRACT No. AF 33(616)-5807
PROJECT No. 7381

AERONAUTICAL SYSTEMS DIVISION
AIR FORCE SYSTEMS COMMAND
UNITED STATES AIR FORCE
WRIGHT-PATTERSON AIR FORCE BASE, OHIO

500 - December 1961 - 11-411 & 412

FOREWORD

This report was prepared by New York University under USAF Contract No. AF 33(616)-5807. The contract was initiated under Project No. 7381, "Materials Application", Task No. 73812, "Data Collection and Correlation". The work was administered under the direction of the Directorate of Materials and Processes, Deputy for Technology, Aeronautical Systems Division, with Lt. William H. Hill and Dr. Ibrahim K. Ebcioglu acting as project engineers.

This report covers work conducted from April 1960 through March 1961.

ABSTRACT

A creep buckling theory is developed based upon fundamental concepts of a mechanical equation of state to represent the time dependent behavior at instability of columns and also a time dependent formulation of the governing differential equation and stability criterion. The predictions of this theory as well as those of other classical stability hypotheses are then correlated with recent experimental data of creep buckling of 2024-0 aluminum alloy columns. A simplified approach for prediction of creep buckling is also presented and this is correlated with test data on columns of various aluminum alloys, titanium alloys, and 17-7PH stainless steel. Conclusions are drawn as to the predictive value of classical stability approaches and to certain important difficulties in correlating the data which are related to the short time failure behavior of columns at elevated temperatures and which seem to have been overlooked in the past.

PUBLICATION REVIEW

This report has been reviewed and is approved.

FOR THE COMMANDER:

W. J. TRAPP
Chief, Strength and Dynamics Branch
Metals and Ceramics Laboratory
Directorate of Materials and Processes

TABLE OF CONTENTS

LIST OF ILLUSTRATIONS

LIST OF ILLUSTRATIONS

(Continued)

LIST OF SYMBOLS

A	column cross sectional area, $in.^2$
C	end fixity coefficient
$\bar{E}$	generalized modulus, psi.
E	modulus of elasticity, psi.
E_r	reduced modulus, psi.
E_s	secant modulus, psi.
E_t	tangent modulus, psi
E_u	defined in Figure 1, psi. min.
I	moment of inertia, in^4.
L	column geometric length, in.
L'	column reduced length, in.
M_i	internal bending resistance, in.lb.
T	temperature, ^oF.
t	time, min.
w	lateral deflection, in.
w_o	central lateral deflection, in.
x	coordinate in loading direction, in.
z	coordinate in lateral direction, in.

LIST OF SYMBOLS

(Continued)

ϵ	strain, microin/in.
ϵ_c	creep component of strain, microin/in.
ϵ_{cr}	critical strain, microin/in.
σ	stress, psi.
σ_a	applied stress, psi.
σ_{cr}	critical stress, psi.
ρ	radius of gyration, in.
φ	equation of state function

Note: The Newtonian convention for indicating time derivatives has been used in this report.

I INTRODUCTION

During the past decade, creep buckling theories have evolved along two main lines that are representative extensions of approaches long used for short-time elastic and inelastic stability analyses. The initial imperfection approach to creep buckling of columns postulates that initial imperfections in geometry or loading grow with time ultimately leading to failure. The classical stability approach hypothesizes that an exchange of stable equilibrium configurations from the straight to the bent form occurs at a critical time at which creep of the column has caused the required reduction of bending stiffness.

For short-time stability, the simplicity and predictive value of classical stability theory has favored its use over the more detailed calculations required by the initial imperfection theories. For the latter, not only must the value of initial imperfection be known or assumed, but the development is further encumbered by the necessity of assuming an explicit form of variable stress creep law. The classical stability approach on the other hand, has the great advantage of not requiring specification of the degree of initial imperfection and further does not require the assumption of an explicit creep law.

The ultimate choice of the classical stability or the initial imperfection theory in engineering problems of creep buckling rests upon the simplest approach to acceptable predictive values. Reliable test data constitute the check of the predictive value of a theory but unfortunately there has been a dearth of such data in the past. The neglect to obtain the basic compressive creep properties of the materials used in the creep buckling tests has often seriously limited the usefulness of the data from the standpoint of correlation with theory.

In this report, a classical stability theory for creep buckling of perfect columns is presented that is based upon certain of the theoretical concepts developed by Rabotnov and Shesterikov(1). The theory is in sufficiently general form that results can be obtained directly from the compressive creep data without requiring fitting of these data with an explicit creep law.

Manuscript released by the authors on May 1, 1961 for publication as a WADC Technical Report.

The predictions of this theory as well as those of other classical stability hypotheses are then correlated with recent experimental data on creep buckling of 2024-0 aluminum alloy columns. Conclusions are drawn as to the predictive value of classical stability approaches and to certain important difficulties in correlating the data which seem to have been overlooked in the past.

II THEORY OF CREEP BUCKLING OF COLUMNS

The Rabotnov-Shesterikov analysis (1) of the creep buckling of perfect columns is of major importance because it is based upon fundamental concepts that logically extend classical stability concepts into the creep regime. Among the concepts utilized are a mechanical equation of state to represent the time-dependent behavior at instability and a time-dependent formulation of the governing differential equations and stability criterion. Each of these concepts is discussed in some detail in the following development and certain modifications of the original concepts are introduced.

1. Equations of State

A perfect column undergoes axial compressive deformation before buckling occurs and therefore follows the appropriate constant stress creep relation. At buckling, an exchange of equilibrium configurations occurs from the straight to the bent form. Hence a variable stress creep law is required to relate the incremental stresses and strains associated with bending in the presence of a relatively large axial compressive strain.

At buckling, Rabotnov and Shesterikov have assumed that a mechanical equation of state in terms of the creep components of strain, ϵ_c, may be used in the following form,

$$\varphi\ (\sigma,\ \epsilon_c,\ \dot{\epsilon}_c,\ T) = 0 \qquad (1)$$

Eq. (1) would seem to be valid for small departures from the initial axially compressed state. It appears, however, that neglect of the elastic strain and strain rate components may not be justified particularly in the region of primary creep.

In fact, many of the phenomenological creep relations that are currently in favor are given in terms of the total strain rate, $\dot{\epsilon}$. As a consequence, the following equation of state has been assumed in the analysis presented herein.

$$\varphi\ (\sigma,\ \epsilon,\ \dot{\epsilon},\ T) = 0 \qquad (2)$$

Eq. (2) implies that creep data may be transformed into constant strain rate stress-strain data in the form shown schematically in Fig. 1 for a constant temperature. It is apparent that Eq. (2) is satisfied at any point on the σ, ϵ, $\dot{\epsilon}$ surface.

For an incremental departure from a point on this surface, representing the bent and initial states, respectively,

$$\delta\ \sigma = (\partial\sigma/\partial\epsilon)\ \delta\epsilon + (\partial\sigma/\partial\dot{\epsilon})\ \delta\ \dot{\epsilon} \qquad (3)$$

In a more convenient form,

$$\delta\sigma = E_t\,\delta\epsilon + E_u\,\delta\dot{\epsilon} \qquad (4)$$

where E_t and E_u represent the local tangents to the φ-surface along the ϵ or $\dot{\epsilon}$ coordinates, respectively.

2. Buckling Models

Before proceeding to the formal analysis, it seems worthwhile to review the buckling models that have been accepted for elastic and inelastic stability of columns. The creep buckling mechanism can then be observed to form a logical evolution of these basic principles.

The fundamental perfect column problem is the determination of the effective bending stiffness after the column has undergone end shortening whether it be elastic, inelastic or creep. Consequently, it is necessary to examine the stress-strain path associated with axial deformation as distinct from that associated with incremental bending. For the simplest case, elastic buckling, the axial deformation follows path OA as shown in Fig. 2a; incremental bending follows AA+ on the concave side and AA- on the convex side. Thus, the elastic modulus is associated with the bending stiffness.

The commonly accepted model for inelastic buckling is illustrated in Fig. 2b. According to the tangent modulus model, axial deformation proceeds along path OA until buckling occurs. At buckling, incremental bending and axial loading proceed simultaneously so that the stress state on the convex side remains at A while the concave side follows path AA+ in the direction of the local tangent modulus.

The last statement implies an assumption concerning the strain rate of infinitesimal bending that was first pointed out in Ref. 2. In order for the path AA+ to be in the direction of the local tangent modulus, loading on the concave side must proceed at a strain rate associated with the compressive stress-strain curve. If this assumption were not implied, but instead instantaneous incremental bending were assumed, then the local bending stiffness would have a value of E and buckling would not occur. Thus, incremental bending at the local strain rate leads to a lower limit to the bending stiffness which appears to be the appropriate value to use in determining instability.

As indicated in Fig. 3, the conditions at inelastic buckling deviate only slightly from those before buckling. Consequently, the value of the tangent modulus is governed by the axial compressive conditions of σ, ϵ and $\dot{\epsilon}$.

In creep buckling, a series of stress-strain curves at different strain rates reflect the time dependent nature of the problem as shown in Fig. 2c. In the presence of an applied compressive stress, it was pointed out in Ref. 2 that the local tangent modulus decreases with time as successive strain rate curves are crossed along path AB until buckling occurs. Thus, for creep buckling as for inelastic buckling the lower bound to the bending stiffness is taken as the tangent modulus appropriate to the strain rate conditions at buckling. In this sense, the creep buckling mechanism is a logical extension of that associated with inelastic buckling.

Shanley (3) has pointed out that even in the presence of a constant axial load, σ_a, the tangent modulus model can be used by assuming that the axial strain increases slightly at buckling to prevent a strain reversal on the convex side of the column. Thus, no part of the column unloads and it is not necessary to use the reduced modulus concept or account for creep recovery effects.

3. Equilibrium Equations

Rabotnov and Shesterikov in Ref. (1) considered the stability of a column subject to creep buckling from both a dynamic and quasi-static point of view with the same result in each case. In the dynamic analysis, the pertinent equations of motion were derived and the stability of the system was determined from the damping characteristics of an infinitesimal lateral oscillation. In the quasi-static treatment, a time dependent equilibrium equation was formulated and the stability was determined from the character of the lateral deflection following the removal of an infinitesimal lateral disturbance.

The essential feature of the creep buckling problem appears in its simplest form in the quasi-static analysis of Ref. 1 and is used in the following together with the equation of state in terms of the total strain, Eqs. (2) to (4).

With the assumption that plane sections remain plane, the incremental bending strain that arises at buckling is given by

$$\delta \epsilon = -z \, \partial^2 w/\partial x^2 \tag{5}$$

By substituting Eq. (5) into (4)

$$\delta \sigma = -E_t z \, (\partial^2 w/\partial x^2) - E_u z \, (\partial^3 w/\partial x^2 \partial t) \tag{6}$$

The internal bending resistance is given by

$$\delta M_i = \int \delta\sigma \, z \, dz \tag{7}$$

Since E_t and E_u remain constant in the presence of an axial compressive stress, Eq. (6) can be substituted into Eq. (7) with the following result

$$\delta M_i = - E_t I \left(\frac{\partial^2 w}{\partial x^2} + \frac{E_u}{E_t} \frac{\partial^3 w}{\partial x^2 \partial t} \right) \tag{8}$$

From equilibrium between the external bending moment and the internal bending resistance

$$\delta M_i = \sigma_a A w \tag{9}$$

By substituting Eq. (8) into (9), the following governing equilibrium differential equation is obtained

$$\frac{\partial^2 w}{\partial x^2} + \frac{E_u}{E_t} \frac{\partial^3 w}{\partial x^2 \partial t} + \frac{\sigma_a}{E_t \rho^2} w = 0 \tag{10}$$

A solution of Eq. (10) can be given in the following form for a simply supported column

$$w = w_o(t) \sin (\pi x/L) \tag{11}$$

By substituting the appropriate derivatives of Eq. (11) into (10),

$$\left[- \left(\frac{\pi}{L}\right)^2 w_o - \frac{E_u}{E_t} \left(\frac{\pi}{L}\right)^2 \dot{w}_o + \frac{\sigma_a}{E_t \rho^2} w_o \right] \sin (\pi x/L) = 0 \tag{12}$$

For a nontrivial solution, the bracketed terms are set equal to zero with the following result

$$\frac{\sigma_a}{E_t (\pi \rho / L)^2} = 1 + \frac{E_u}{E_t} \frac{\dot{w}_o}{w_o} \tag{13}$$

In order to complete the problem it is now necessary to introduce a stability criterion that is associated with the lateral deflectional response $\dot{w}_o/w_o$.

4. Stability Criterion

The stability investigation of an elastic or inelastic column consists of applying an infinitesimal lateral disturbance at the critical load to determine if the bent form vanishes or remains upon removal of the disturbance. For the creep buckling case, the lateral disturbance is time dependent according to Eq. (11) and therefore a revised stability criterion must be introduced.

In Ref. 1, the character of the lateral deflectional response was shown to be as follows:

$\dot{w}_o/w_o$	lateral deflection	
+	increasing	unstable
0	constant	neutral
-	decreasing	stable

Thus, the condition of $\dot{w}_o/w_o = 0$ was taken as the stability criterion for creep buckling of the column and it is from this that the quasi-static analysis derives its name. With this criterion, Eq. (13) reduces to

$$\sigma_a = E_t(\pi\rho/L)^2 \tag{14}$$

It is interesting to note that a similar result was suggested in Ref. 2 on an intuitive basis. Since σ_a and L/ρ are prescribed in this case, creep buckling of the column occurs when E_t has reduced sufficiently through creep to satisfy Eq. (14). The critical time can be obtained through use of Eq. (2) as is shown in the next section.

III DEVELOPMENT OF CREEP BUCKLING RESULTS

In this section, our purpose is to demonstrate the use of the theory developed in Section II for the prediction of creep buckling times of aluminum alloy 2024-0 columns at 500^{o} F. The results of tests on such columns have previously been reported in reference (5). Compressive creep data obtained in the experimental program and previously shown in Figure 5 of reference (5) are used in this section for the development of the theoretical results. In addition, the compressive data are used to evaluate other approaches to the creep buckling of perfect columns that have been suggested previously.

1. Constant Strain Rate Theory

As a first step in the development of theoretical results, the compressive creep data are transformed graphically into constant strain rate stress-strain data, as implied by Eq. (2), by a series of steps. From the latter, E_t in Eq. (14) can then be evaluated. Further, by an inverse sequence, the critical times are found graphically from the compressive creep curves. The entire development is illustrated in the following.

The tangents to the compressive creep curves in Figure 4 represent the instantaneous values of strain rate. The strain rates for each creep curve may now be plotted as a function of strain as shown in Figure 5. The intersections of the curves with any vertical in Figure 5 represent the stress and strain data at a constant strain rate. It is now possible to construct constant strain rate stress-strain curves for any specified strain rate using these data as shown in Figure 6. Also included in Figure 6 is the short time compressive stress-strain curve with a strain rate of approximately 50,000 microin/in/min.

In order to apply Eq. (14) conveniently, the tangent moduli to the curves given in Figure 6 are now determined and plotted against stress as shown in Figure 7. A straight line through the origin on this graph is associated with a particular slenderness ratio column since from Eq. (14) for simply supported columns

$$(\pi\rho/L)^2 = \sigma_a/E_t \tag{15}$$

It is possible to generalize Eq. (15) for other boundary conditions by the introduction of the reduced length L' where

$$L' = L/C^{1/2} \tag{16}$$

Hence Eq. (15) becomes transformed into

$$(\pi\rho/L')^2 = \sigma_a/E_t \tag{17}$$

Eq. (17) defines the slope of the line through the origin. Two such lines for $L'/\rho = 40$ and $L'/\rho = 60$ are shown in Figure 8 which is simply the lower portion of Figure 7 drawn to a larger scale. Each intersection of such a line with a constant strain rate-tangent modulus curve represents an unique set of conditions for creep buckling. The implication is that for the particular applied stress the column will buckle when the tangent modulus which is associated with the bending stiffness of the column reaches the appropriate value of Figure 8.

It is most convenient to find strain rates corresponding to the correct tangent modulus for specific L'/ρ values from a cross plot of the data in Figure 8 in terms of stress and strain rate as shown in Figure 9 for $L'/\rho = 40$ and $L'/\rho = 60$. Each curve in the figure represents the variation of strain rate values with stress for the indicated slenderness ratio.

In order to predict creep buckling times, one first finds the appropriate strain rate for the applied stress and L'/ρ value from Figure 9. The creep strain corresponding to the strain rate is then found from Figure 5 and the creep buckling time can be read off from the proper compressive creep curve in Figure 4. It should be noted that the critical time so determined is for creep buckling of a perfect column.

Using the process just described, critical times were found for a number of applied stresses for $L'/\rho = 40$ and these are given in Table 1 as the $E_t(\dot{\epsilon})$ analysis. In the table the actual values of applied stress are given as well as the stresses normalized to the theoretical short time tangent modulus buckling stress. The latter was computed using the short time compressive creep properties at 500°F which were previously reported in reference (5) and shown here in Figure 6.

It was not possible to complete the analysis for $L'/\rho = 60$ columns since the required low stress level creep curves were not available.

TABLE 1 - THEORETICAL CREEP BUCKLING RESULTS FOR $L'/\rho = 40$ ALUMINUM ALLOY 2024-0 COLUMNS AT 500°F.

Theoretical Analysis	Applied Stress σ_a psi	Normalized Stress σ_a/σ_{cr}	Strain Rate, $\dot{\epsilon}$ microin/in/min	Strain, ϵ microin/in	Critical Time t_{cr}, min.
$E_t(\dot{\epsilon})$	8500	1.00	50000	1800	approx. 0.1
	7165	.84	4200	1060	0.25
	6320	.74	590	1380	1.0
	5480	.64	86	1320	4.0
$E_r(\dot{\epsilon})$	9250	1.00	50000	2600	approx. 0.1
	7587	.83	1700	2400	.4
	7165	.77	500	2770	2.0
	6744	.73	205	3000	4.5
	6320	.68	64	3160	15.0
$E_t(t)$	8500	1.00			approx. 0.1
	6320	.74			1.4
	5480	.64			6.0
$E_r(t)$	9250	1.00			approx. 0.1
	7180	.78			5.0
	7050	.76			10.0
	6770	.73			20.0
	6590	.71			40.0
E_s	10850	1.00		6180	approx. 0.1
	8500	.78		6180	1.3
	8000	.74		6180	3.5
	7587	.70		6180	7.3
	7165	.66		6180	22.0
	6744	.62		6180	49.0

TABLE 2 - THEORETICAL CREEP BUCKLING RESULTS FOR $L'/\rho = 60$ ALUMINUM ALLOY 2024-0 COLUMNS AT 500°F.

Theoretical Analysis	Applied Stress σ_a psi	Normalized Stress σ_a/σ_{cr}	Strain Rate, $\dot{\epsilon}$ microin/in/min	Strain, ϵ microin/in	Critical Time t_{cr}, min.
E_r ($\dot{\epsilon}$)	8150	1.00	50000	1550	approx. 0.1
	6744	.83	3200	1200	.4
	6320	.78	530	1420	1.1
	5480	.67	76	1300	3.5
E_s	9380	1.00		2740	approx. 0.1
	7587	.81		2740	0.7
	7165	.76		2740	1.9
	6744	.72		2740	3.3
	6320	.67		2740	9.4
	5480	.58		2740	39.5

For reasons to be discussed subsequently, it is of interest to repeat the above analysis with the reduced modulus, E_r, substituted in Eq. (17) for the tangent modulus. The reduced modulus is defined as

$$E_r = 4EE_t/[\ (E)^{1/2} + (E_t)^{1/2}\ ]^2 \qquad (18)$$

Using the tangent modulus data obtained from the short time compressive stress-strain curve, Eq. (18) was evaluated and the strain rate values were plotted against stress as shown in Figure 10 for $L'/\rho = 60$. The critical times were found using the procedures previously described and are given in Tables 1 and 2 as the $E_r(\dot{\epsilon})$ analysis.

2. Other Creep Buckling Hypotheses

Isochronous compressive stress-strain curves, shown in Figure 11, were derived from the compression creep data also. These data were analyzed to find creep buckling times for $L'/\rho = 40$ columns using the Shanley hypothesis (3). In addition a Shanley type analysis in which the reduced modulus was substituted for the tangent modulus was also performed. The numerical results are given in Table 1 as the $E_t(t)$ and $E_r(t)$ analyses.

As a simple approach to the creep buckling of columns, Gerard (4) hypothesized that a time dependent secant modulus could be used to determine critical strain. The critical time could then be found directly from the compressive creep curves for any applied stress. If buckling is governed by

$$\sigma_{cr} = \pi^2 E_s/(L'/\rho)^2 \qquad (19)$$

and since the secant modulus is given by

$$E_s = \sigma/\epsilon \qquad (20)$$

Then, by combining Eq. (19) and Eq. (20)

$$\epsilon_{cr} = (\pi\rho/L')^2 \qquad (21)$$

Critical time values using Eq. (21) directly with the creep curves are given in Tables 1 and 2 for $L'/\rho = 40$ and $L'/\rho = 60$ respectively as the E_s analysis.

A comparison of the predicted creep buckling times of the various theories has been shown for normalized applied stresses for $L'/\rho = 40$ columns in Figure 12. The use of the normalized stress allows a more rational comparison among theories with different short time buckling stress which vary from 8500 psi (tangent modulus theory) to 10,850 psi (secant modulus theory). The various theories which have been evaluated here are correlated with test data in the next section.

IV CORRELATION OF THEORY WITH EXPERIMENTS

In this section correlation of the various theories with test data is considered under three separate categories:

1. Short time buckling theories.
2. Constant strain rate creep buckling theory as developed in Sections II and III of this report.
3. Comparison of various theories with test data to assess their relative predictive value.

1. Short Time Buckling

Experimental results reported in reference (5) and shown herein in Figure 13 indicate that the short time failure strength of columns of aluminum alloy 2024-0 at 500°F are consistently higher than the critical stresses predicted by the tangent modulus theory. The short time test data of reference (5) are shown in Figure 13 relative to the tangent modulus, reduced modulus and secant modulus theories as evaluated from the following relation

$$\sigma_{cr} = \pi^2 \bar{E}/(L'/\rho)^2 \qquad (22)$$

In each case, the appropriate moduli were derived from the short time compressive stress strain curve of aluminum alloy 2024-0 at 500°F shown in Figure 6.

In discussing the test data presented in Figure 13, it is important to identify the effective initial imperfections present in the columns. As a consequence, load-central deflection data were obtained during each of the experiments at the test temperature. Southwell analyses of these data indicated the effective initial imperfections were less than 4 percent of the column thickness for pin end columns and were less than 1 percent for fixed end columns.

The data in Figure 13 do not correlate with any one short time theory. Rather, for the pin end columns with their higher initial imperfections, the tangent modulus theory appears to form a lower bound while the reduced modulus theory is an upper bound. For the fixed end columns, the failure strengths are higher apparently as a result of the smaller initial imperfections and the reduced modulus and secant modulus form the lower and upper bounds, respectively. It is important to note that a similar discrepancy between the test data and tangent modulus theory can be observed from tests of others. Short time failure strength data at elevated temperatures for pin end columns given in references (6) and (7) fall between the tangent modulus stress and the secant modulus stress.

To explain the observed discrepancy between test data and tangent modulus theory at 500°F, it is important to return for a moment to the room temperature situation. Here, it is an experimental fact that the experimental failure strength of aluminum alloy columns containing small initial imperfections coincides rather closely with the theoretical tangent modulus stress for a perfect column. This fact depends to some extent upon the stress strain characteristics of the column material.

At elevated temperatures such as 500°F, it is believed that the stress strain characteristics of the column material are sufficiently reduced that the failure strength of the column can significantly exceed the tangent modulus stress. This hypothesis is supported in part by the analysis presented in reference (8) as well as the test data presented in Figure 13 and references (6) and (7). It appears that a reexamination of the short time buckling characteristics of inelastic columns at elevated temperatures is required to explain the experimental observations.

2. Constant Strain Rate Creep Buckling

Results obtained from the constant strain rate creep buckling theory, $E_t(\dot{\epsilon})$, developed in Sections II and III are shown in Figure 14 for columns of $L'/\rho = 40$. These results are shown in conjunction with creep buckling test data on pin end and fix end columns. Also included for reference are the constant strain rate reduced modulus results, $E_r(\dot{\epsilon})$, as well as the secant modulus results, E_s.

It is quite apparent that the trend predicted by any of the theoretical lines in Figure 14 is in reasonable agreement with the trend of the test data in each grouping. The major source of discrepancy appears to be related to the short time behavior. Note that the discrepancy between the short time test data and the $E_t(\dot{\epsilon})$ line, for example, appears to be preserved out into the creep buckling region. A shifting upward of this line to eliminate the discrepancy for short time buckling would likewise eliminate the discrepancy for creep buckling.

There appear to be striking similarities between the short time behavior shown in Figure 13 and the creep buckling behavior shown in Figure 14. In both, the test data for the pin end columns (C=1) are bounded by the tangent and reduced modulus results while the data for the fixed end columns (C= 3.75) are bounded by the reduced and secant moduli. Thus, the results suggest a distinct dependence of the creep buckling behavior upon the short time buckling characteristics.

Similar observations can be made for $L'/\rho = 60$ columns of aluminum alloy 2024-0 at 500°F as shown in Figure 15. The constant strain rate-tangent modulus curve is not shown in this figure since compressive creep curves at sufficiently low stress levels were not available and hence a complete analysis for this slenderness ratio could not be made. However, the tangent modulus curve would appear in the same relative position in Figure 15 as it does in Figure 14.

3. Comparison of Various Approaches to Creep Buckling

A rational comparison of various perfect column approaches to creep buckling can be made if short time effects are suppressed in view of the apparent dependence of creep buckling upon the short time buckling behavior. This can be accomplished by normalizing the theoretical creep buckling stresses to the appropriate short time theoretical critical stresses and by normalizing the applied stresses to the appropriate short time failure strengths for the experiments. Such a normalized representation is shown in Figure 16 for aluminum alloy 2024-0 columns at 500°F and $L'/\rho = 40$, and in Figure 17 for the $L'/\rho = 60$ data.

It should be noted that with the normalized representation given in Figures 16 and 17, the discrepancies between theory and experiment can be better evaluated and the difference in creep buckling behavior between pin end and fixed end columns disappears. Also the apparent scatter, shown in the standard representation in Figures 14 and 15 is significantly reduced when the data are shown in normalized form.

In Figure 16, all five perfect column approaches to creep buckling, discussed in Section III have been evaluated. The tangent modulus, based either upon the constant strain-rate or upon the isochronous data, appears to serve as a lower bound for creep buckling. The constant strain rate-reduced modulus and the secant modulus approaches appear to correlate most closely with the test data while the isochronous reduced modulus gives values which are somewhat optimistic. The close correlation between the constant strain rate-reduced modulus and the secant modulus approaches with test data is also evident in the results for $L'/\rho = 60$ columns as shown in Figure 17 for the data of reference (5).

In order to demonstrate that the correlation between theory and test data obtained in the present investigation is not unique, the test data of references (6) and (7) were analyzed. These data were obtained on aluminum alloy 2024-T4 columns of $L'/\rho = 31$, 53 and 70 at 350°, 400° and 450°F for creep buckling times up to 300 hours; stainless steel columns of 17-7 PH of $L'/\rho = 61$ and 63 at 775°F up to 100 hours; and titanium alloy RC-130A columns of $L'/\rho = 66$ at 700° and 800°F up to 60 hours.

In this program, the compressive creep characteristics of the column material were obtained and hence the test data were compared to the isochronous tangent modulus as shown by the dashed lines in Figures 18 and 19. Also shown in these figures by the solid lines are the secant modulus results calculated from the compressive creep data of references (6) and (7).

The interesting observation apparent from Figures 18 and 19 is that the secant modulus approach is significantly in better agreement with the test data than the isochronous tangent modulus. The reason is much the same as that concluded previously: the secant modulus is in better agreement with the short time buckling test results and this agreement is preserved out into the creep buckling regime.

As a final demonstration of the applicability of the secant modulus approach, test data for $L'/\rho = 40$ columns of heat treated Ti-7Al-4Mo titanium alloy at 950°F from reference (9) were analyzed. This alloy at 950°F has high compressive yield strength, a sharp knee in the compressive short time stress-strain curve and resistance to creep deformation and is distinctly different in character from the aluminum alloys. The creep buckling data are shown in normalized form in Figure 20 together with the secant modulus results calculated from the compressive short time and creep data of reference (9). In terms of stress the agreement is quite good, despite the previously reported scatter of both the compressive creep properties and the creep buckling times.

V CONCLUSIONS

A rather significant conclusion that is apparent from the test data analyzed herein for the 2024-0 aluminum alloy columns as well as the data for 2024-T4 aluminum alloy, 17-7 PH stainless steel and RC-130A titanium alloy columns obtained by other investigators is concerned with the short time column strength at elevated temperatures. It appears that the elevated temperature failure strength of columns can significantly exceed the corresponding tangent modulus stress. Such results obtained for both pin end and fix end columns are in better agreement with the reduced modulus and often approach the secant modulus stress. As a consequence of this short time behavior, it is necessary to correlate creep buckling theory with test data on a nondimensional basis.

Of the various approaches to creep buckling of perfect columns that have been considered herein, only the constant strain rate theory presented in Section II can be considered to have a theoretical foundation in a formal sense. Consequently, it is of some importance to draw conclusions relative to this theory.

Normalized creep buckling test results on 2024-0 aluminum alloy columns at 500^{o}F are bounded on the lower side by the strain rate tangent modulus and on the upper side by the strain rate reduced modulus. It would appear that the tangent modulus is associated with the development of significant lateral deflections of the column and that the reduced modulus is associated with failure or collapse of the column. Thus, it is concluded that perfect column creep buckling theory has distinct predictive value for columns containing small initial imperfections.

As for the other approaches, the isochronous tangent modulus hypothesis of Shanley is in close agreement with the strain rate tangent modulus. Thus, it too forms a lower bound for the normalized test data on aluminum alloy 2024-0 columns. The secant modulus approach is in close agreement with the strain rate reduced modulus. Consequently, it forms an upper bound for the test data under consideration.

The results and conclusions of this investigation suggest that short time elevated temperature tests of columns are required to establish a base point for creep buckling predictions. Using this base point, any of the normalized creep buckling approaches discussed above may be utilized to construct absolute creep buckling predictions. For a conservative estimate, the strain rate or isochronous tangent modulus may be used. To estimate an upper bound, the secant modulus appears to provide a particularly simple approach.

VI BIBLIOGRAPHY

1. Rabotnov, G. N., and Shesterikov, S. A., "Creep Stability of Columns and Plates," Journal of the Mechanics and Physics of Solids, Vol. 6, pp. 27-34, 1957.

2. Gerard, G., "Note on Creep Buckling of Columns," Journal of the Aeronautical Sciences, Vol. 19, No. 10, p. 714, Oct. 1952.

3. Shanley, F. R., Weight-Strength Analysis of Aircraft Structures, McGraw-Hill Book Co., New York, 1952, p. 349.

4. Gerard, G., "A Creep Buckling Hypothesis," Journal of the Aeronautical Sciences, Vol. 23, No. 9, pp. 879-882, Sept. 1956.

5. Papirno, R. and Gerard, G., "Investigation of Creep Buckling of Columns and Plates Part III: Creep Buckling Experiments with Columns of 2024-0 Aluminum Alloy," WADC TR 59-416 Part III, March, 1961.

6. Carlson, R. L. and Manning, G. K., "Investigation of Compressive-Creep Properties of Aluminum Columns at Elevated Temperatures Part III: Comparisons with Other Metals," WADC TR 52-251, Part III, May, 1955.

7. Carson, R. L., Bodine, E. G. and Manning, G. K., "Investigation of Compressive-Creep Properties of Aluminum Columns at Elevated Temperatures Part 4: Additional Studies," WADC TR 52-251, Part 4, April, 1956.

8. Wilder, T. W., Brooks, W. A., and Mathauser, E. E., "The Effect of Initial Curvature on the Strength of an Inelastic Column," NACA TN 2872, Jan. 1953.

9. Papirno, R. and Gerard, G., "Investigation of Creep Buckling of Columns and Plates Part II: Creep Buckling Experiments with Columns of Ti-7Al-4Mo Titanium Alloy," WADC TR 59-416 Part II, July, 1960.

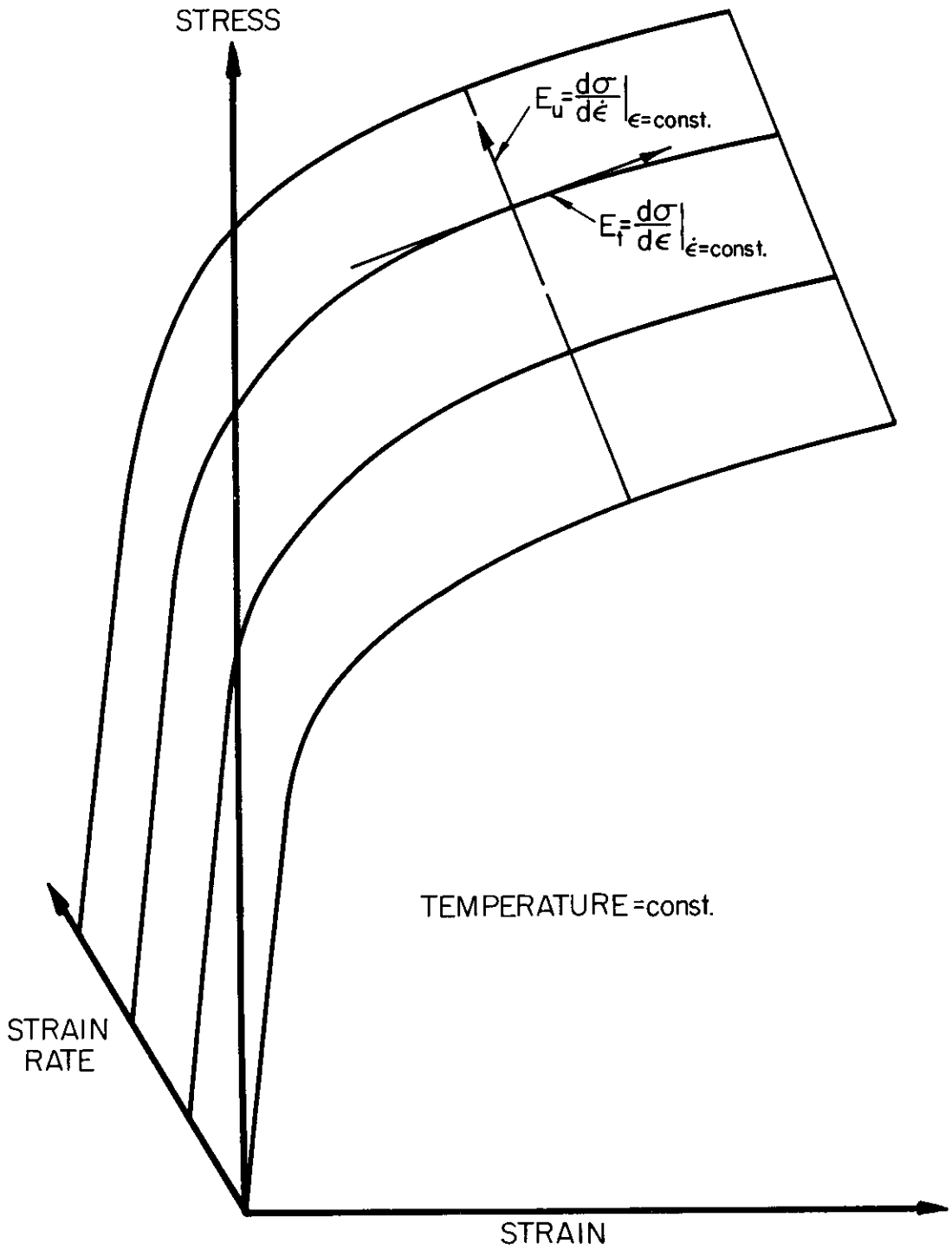

FIGURE 1 STRESS-STRAIN-STRAIN RATE SURFACE FOR A MATERIAL AT A GIVEN TEMPERATURE

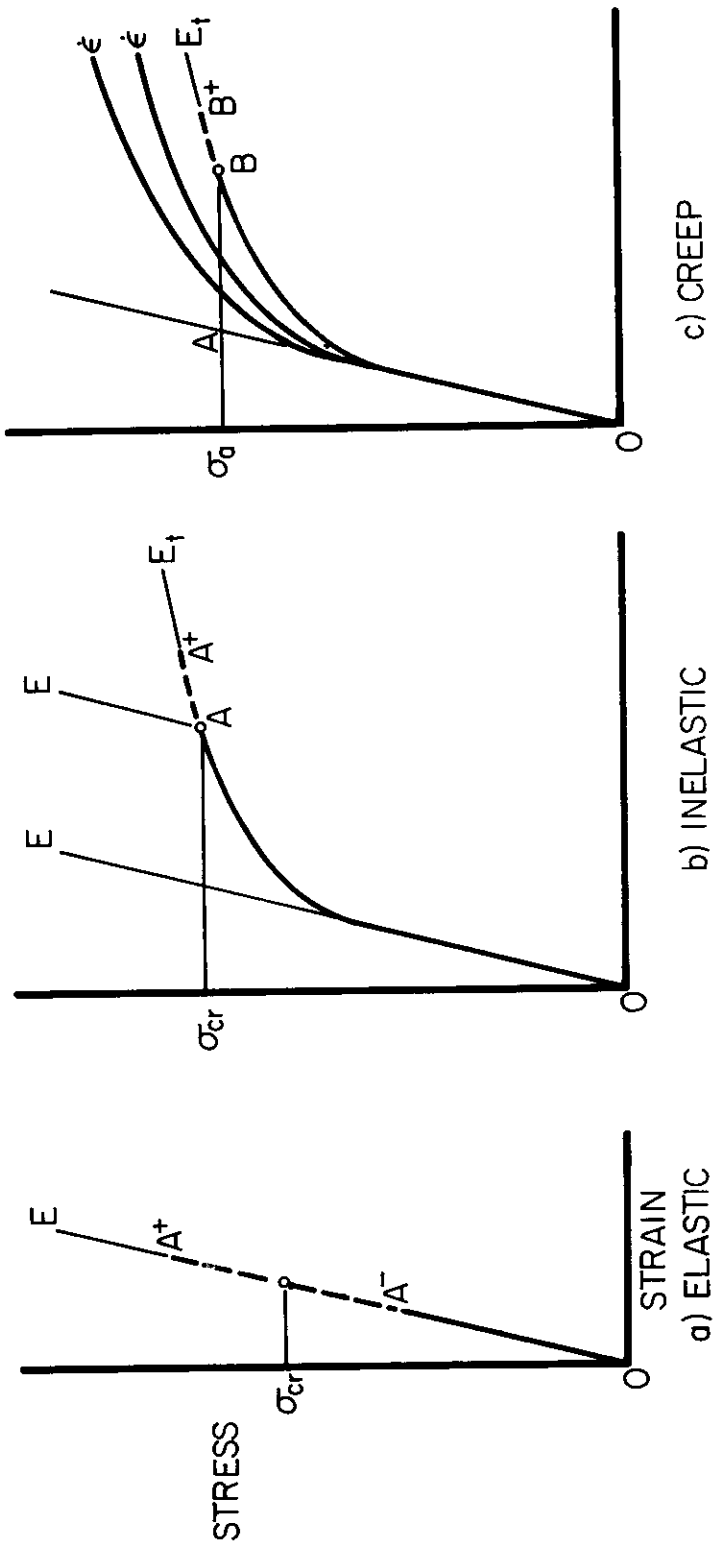

FIGURE 2 MODELS OF BUCKLING BEHAVIOR

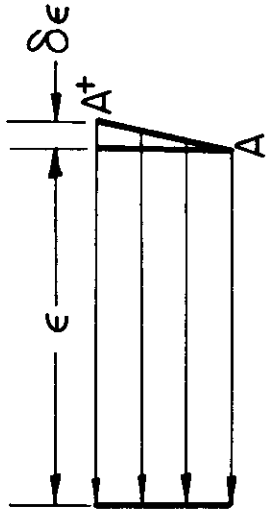

FIGURE 3 STRAIN CONDITIONS IN INELASTIC BUCKLING

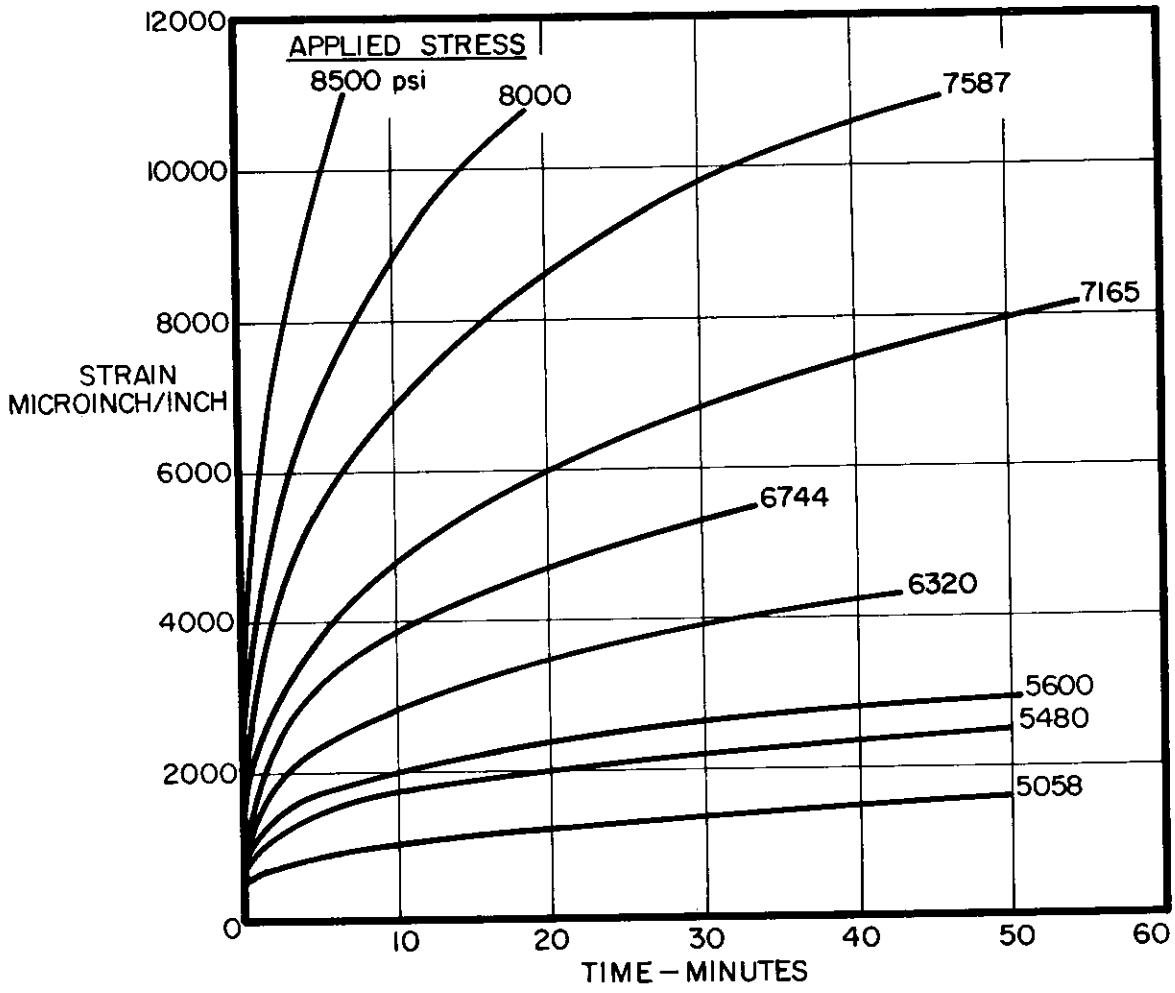

FIGURE 4 AVERAGE COMPRESSION CREEP CURVES FOR 2024-0 ALUMINUM ALLOY AT 500°F

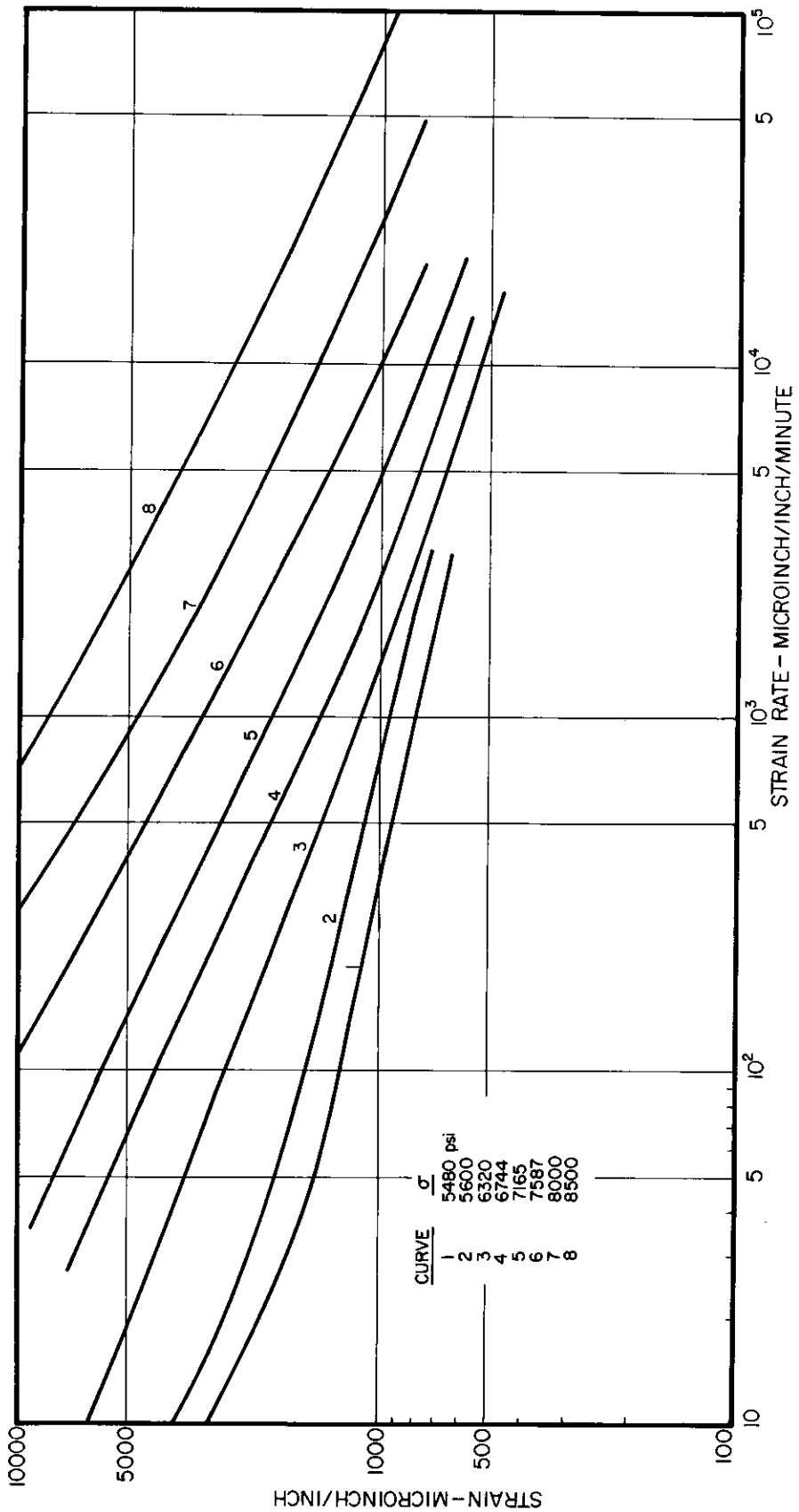

FIGURE 5 STRAIN-STRAIN RATE CURVES FOR 2024-0 ALUMINUM ALLOY AT 500°F

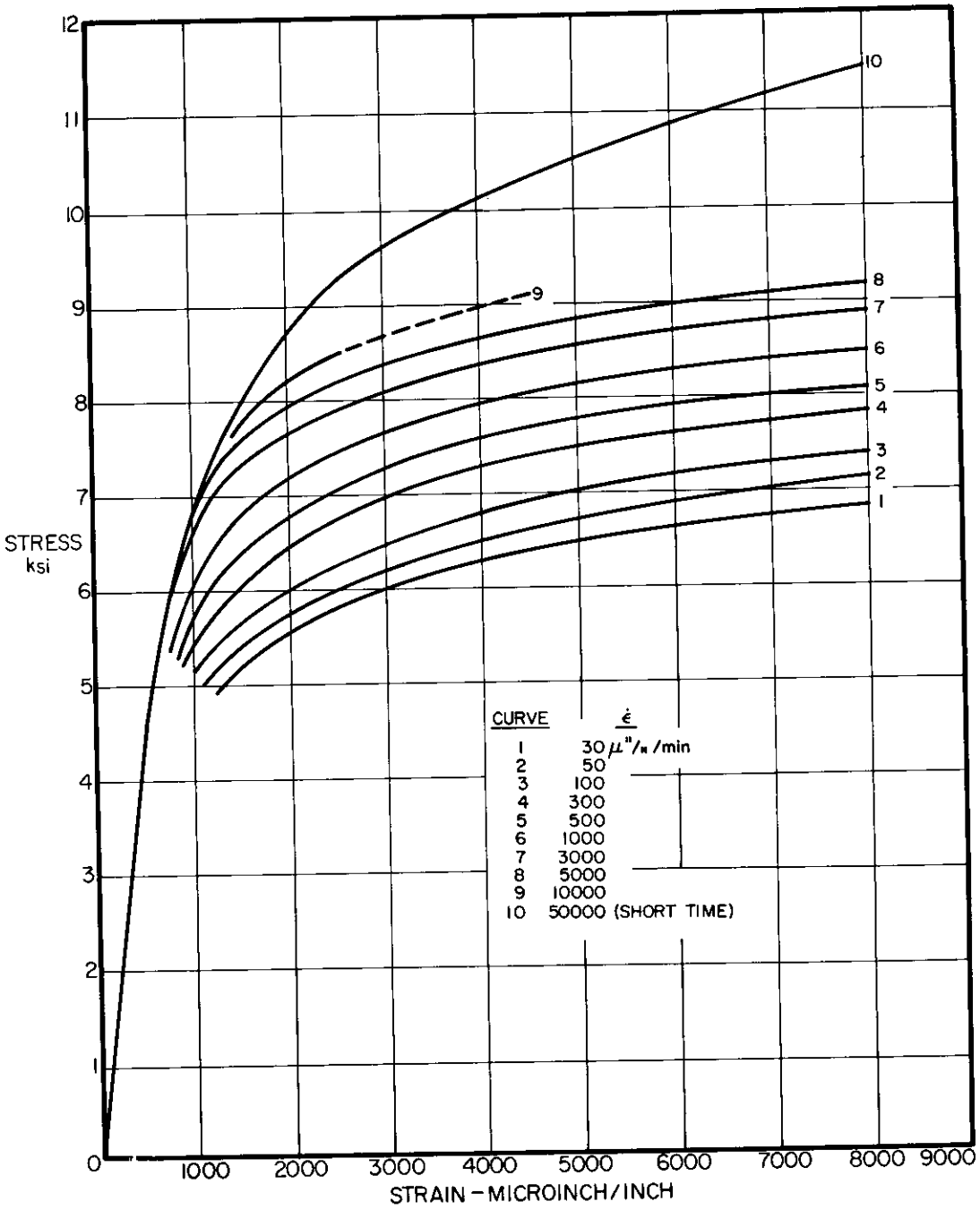

FIGURE 6 CONSTANT STRAIN RATE STRESS-STRAIN CURVES FOR 2024-0 ALUMINUM ALLOY AT 500°F

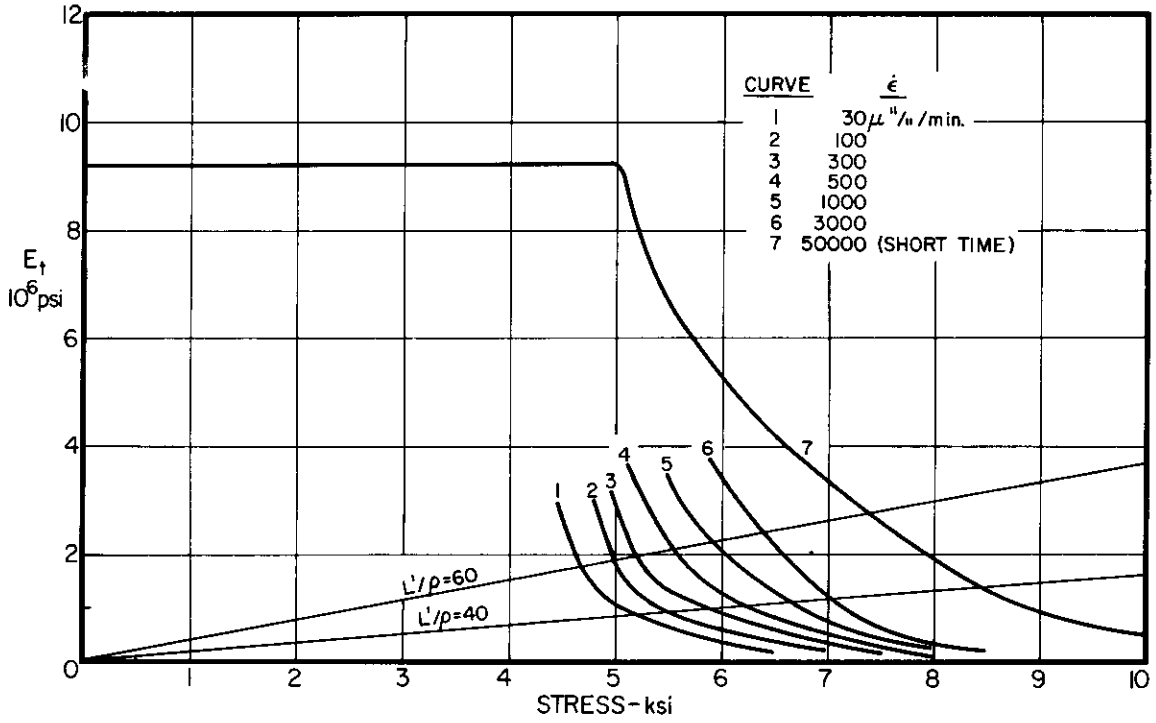

FIGURE 7 TANGENT MODULUS-STRESS CURVES AT CONSTANT STRAIN RATES FOR ALUMINUM ALLOY 2024-0 AT 500°F. (DERIVED FROM DATA IN FIGURE 6)

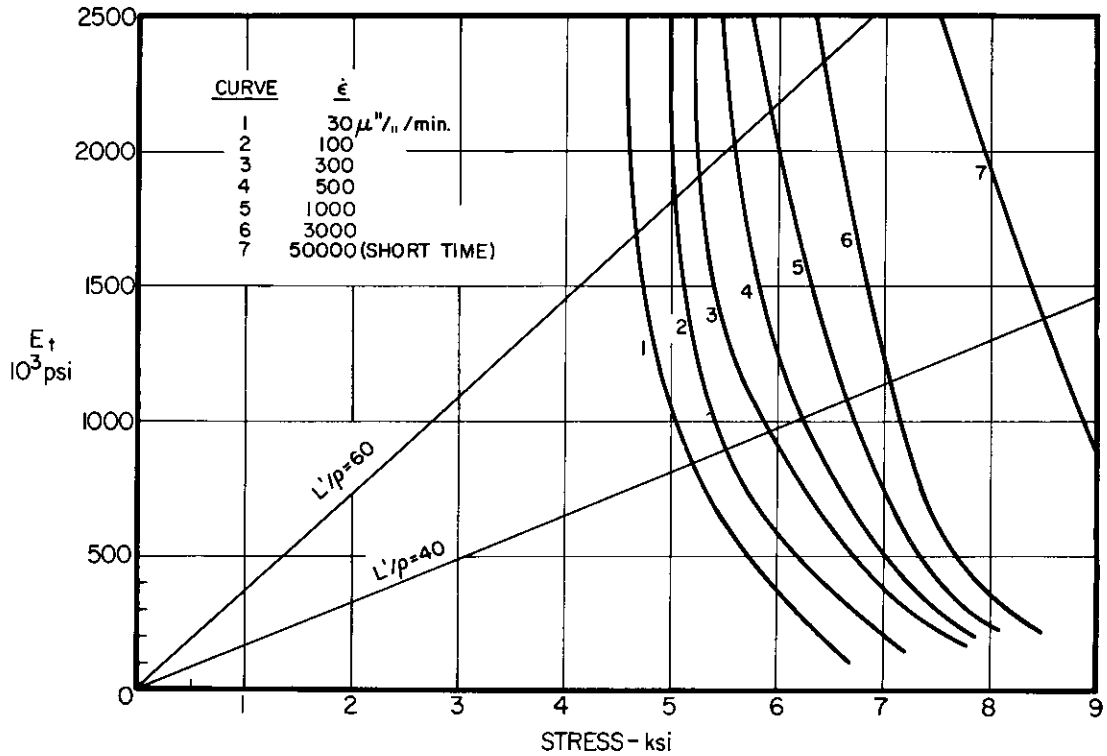

FIGURE 8 TANGENT MODULUS-STRESS CURVES AT CONSTANT STRAIN RATES DRAWN TO LARGER SCALE

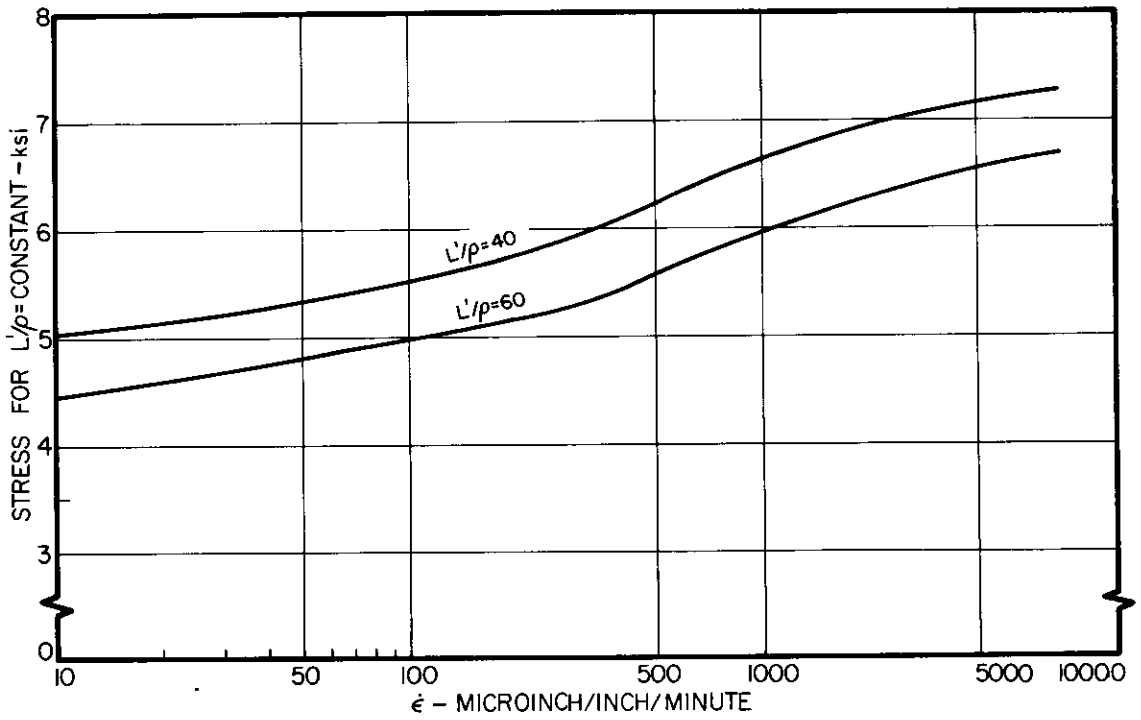

FIGURE 9 INTERPOLATION CURVES FOR CONSTANT STRAIN RATE TANGENT MODULUS THEORY

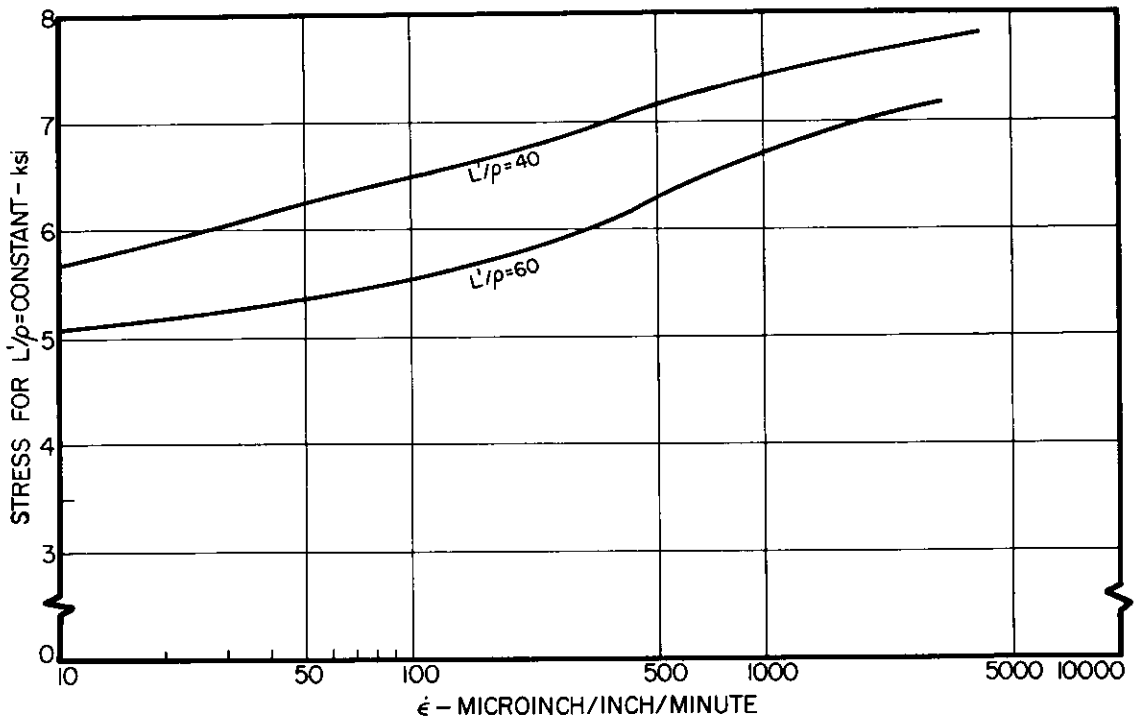

FIGURE 10 INTERPOLATION CURVES FOR CONSTANT STRAIN RATE-REDUCED MODULUS THEORY

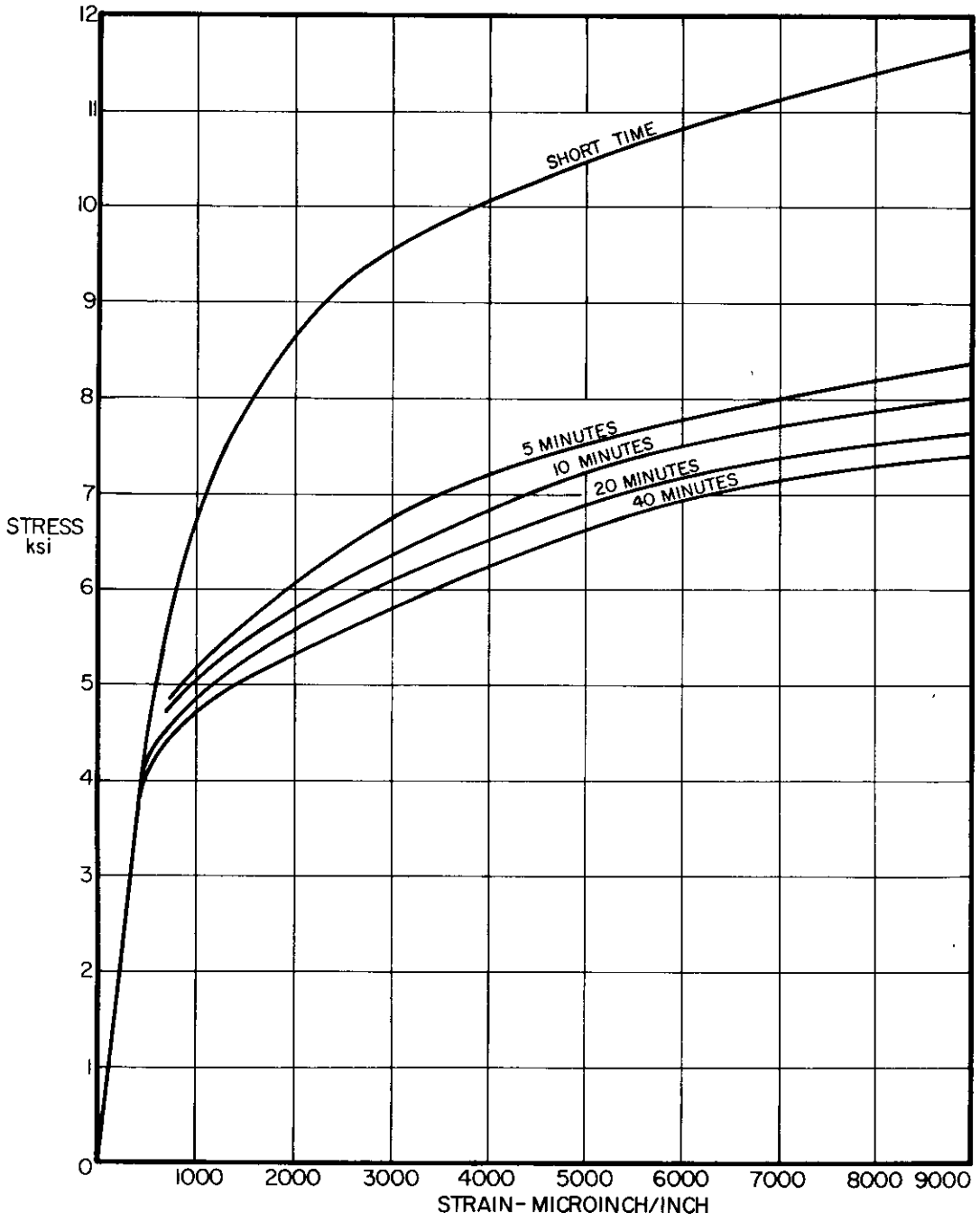

FIGURE 11 ISOCHRONOUS CURVES FOR ALUMINUM ALLOY 2024-0 AT 500°F

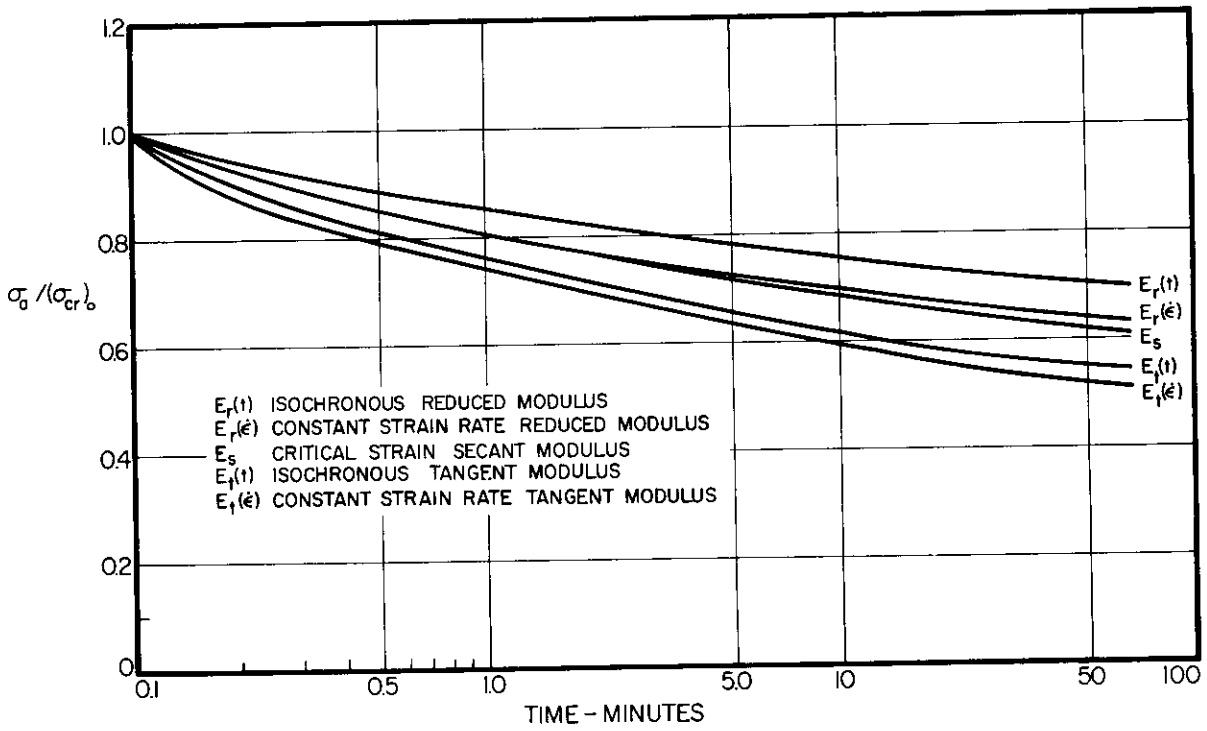

FIGURE 12 COMPARISON OF VARIOUS APPROACHES TO CREEP BUCKLING SHOWN IN NORMALIZED STRESS FORM FOR ALUMINUM ALLOY 2024-0 COLUMNS, $L'/\rho = 40$, at $500^{\circ}F$

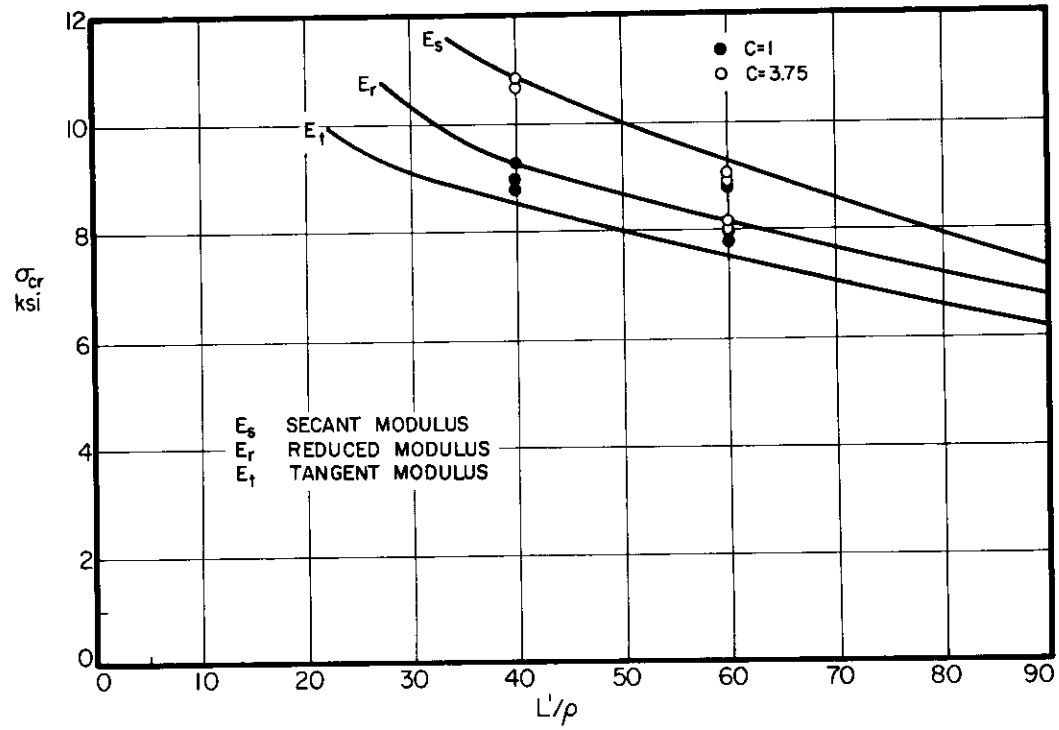

FIGURE 13 CORRELATION OF SHORT TIME BUCKLING THEORY WITH EXPERIMENTS ON ALUMINUM ALLOY 2024-0 COLUMNS AT $500^{\circ}F$

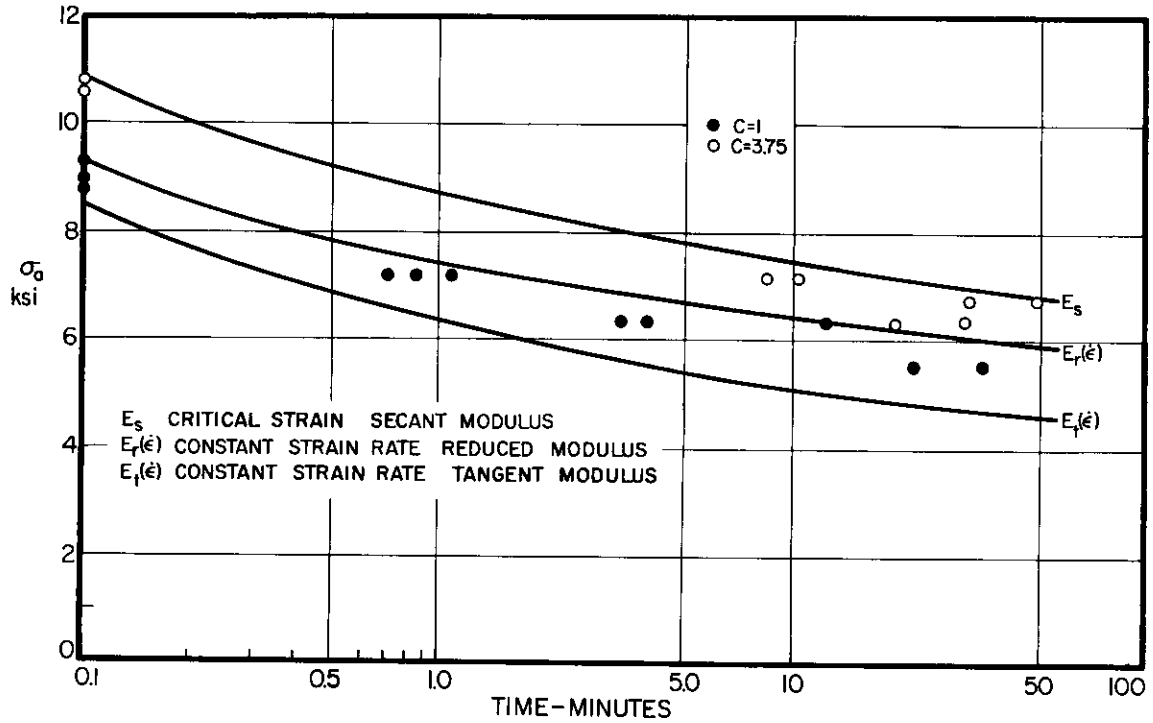

FIGURE 14 CORRELATION OF CONSTANT STRAIN RATE THEORIES AND SECANT MODULUS HYPOTHESIS FOR CREEP BUCKLING WITH EXPERIMENTS ON ALUMINUM ALLOY 2024-0 COLUMNS, $L'/\rho = 40$, AT 500°F

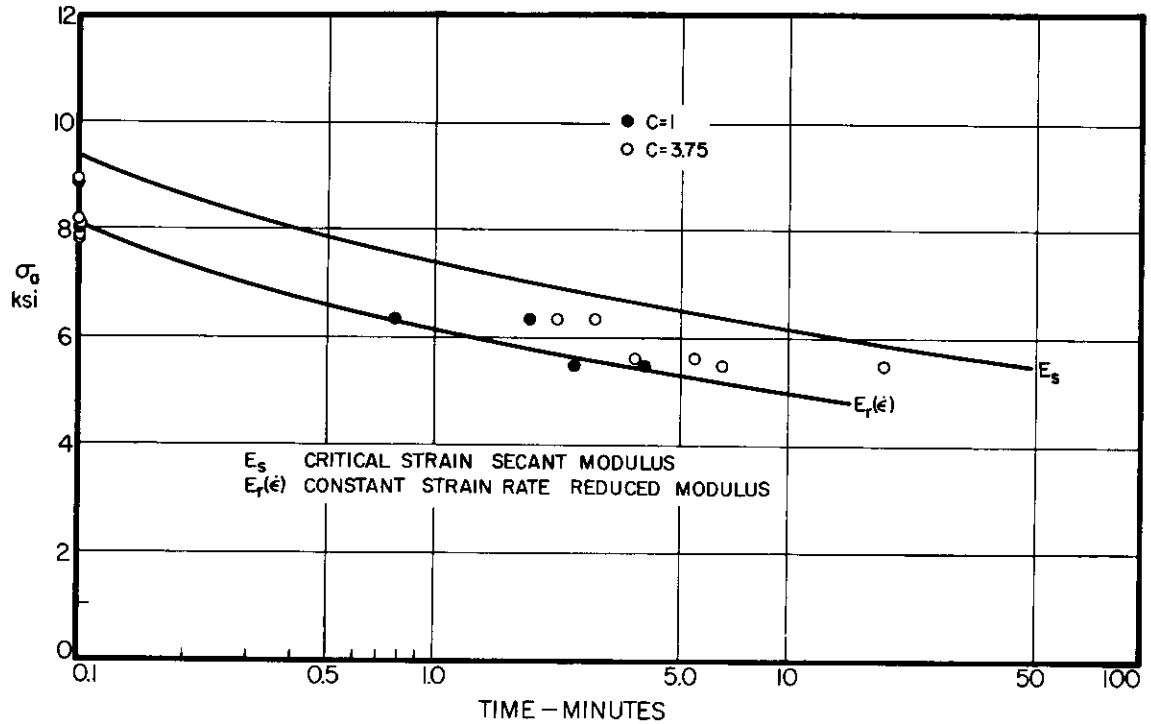

FIGURE 15 CORRELATION OF CONSTANT STRAIN RATE-REDUCED MODULUS THEORY AND SECANT MODULUS HYPOTHESIS FOR CREEP BUCKLING WITH EXPERIMENTS ON ALUMINUM ALLOY 2024-0 COLUMNS, $L'/\rho = 60$, AT 500°F

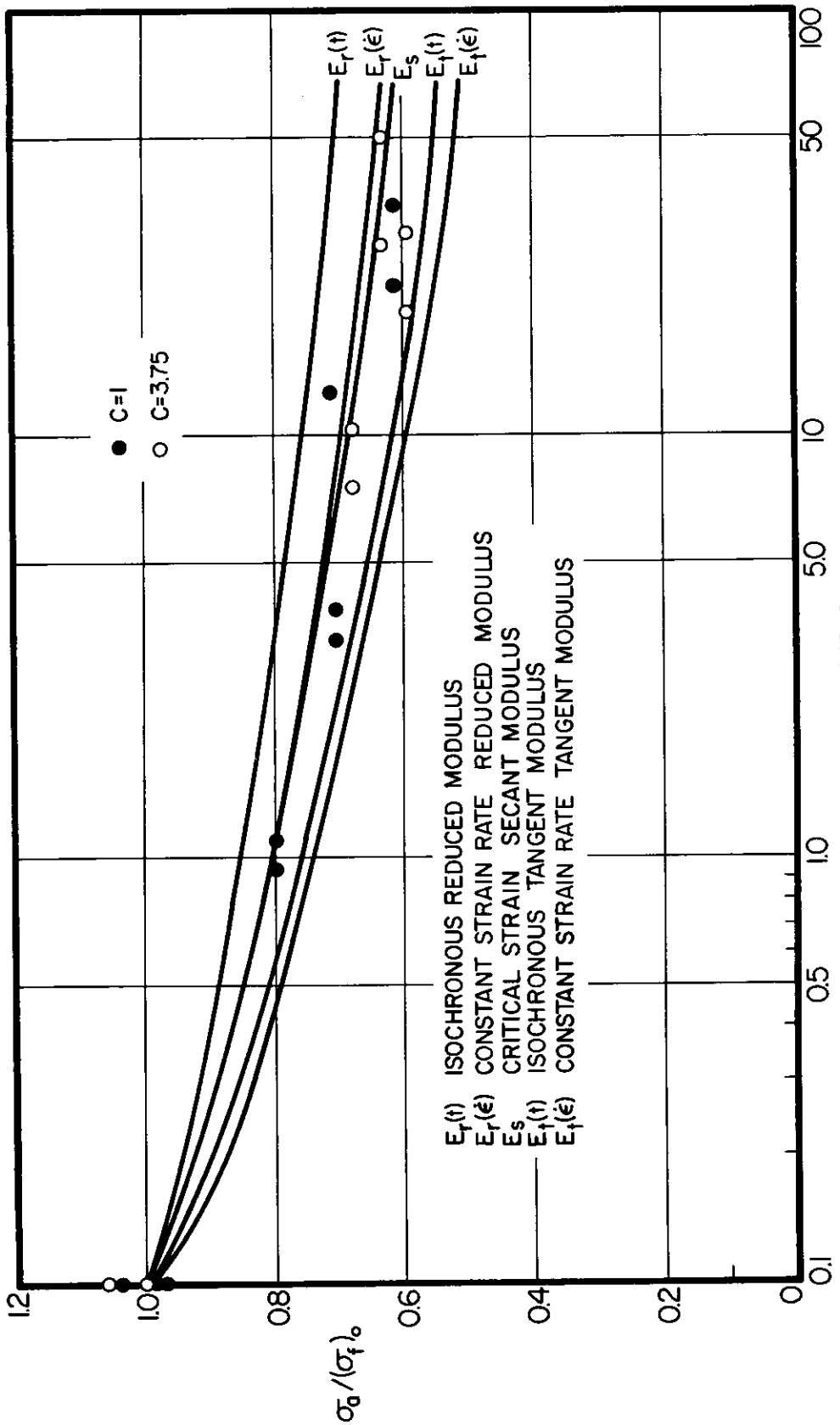

FIGURE 16 CORRELATION OF VARIOUS PERFECT COLUMN THEORETICAL APPROACHES TO CREEP BUCKLING EXPRESSED IN NORMALIZED STRESS FORM WITH EXPERIMENTS ON ALUMINUM ALLOY 2024-0 COLUMNS, $L'/\rho = 40$, AT 500°F

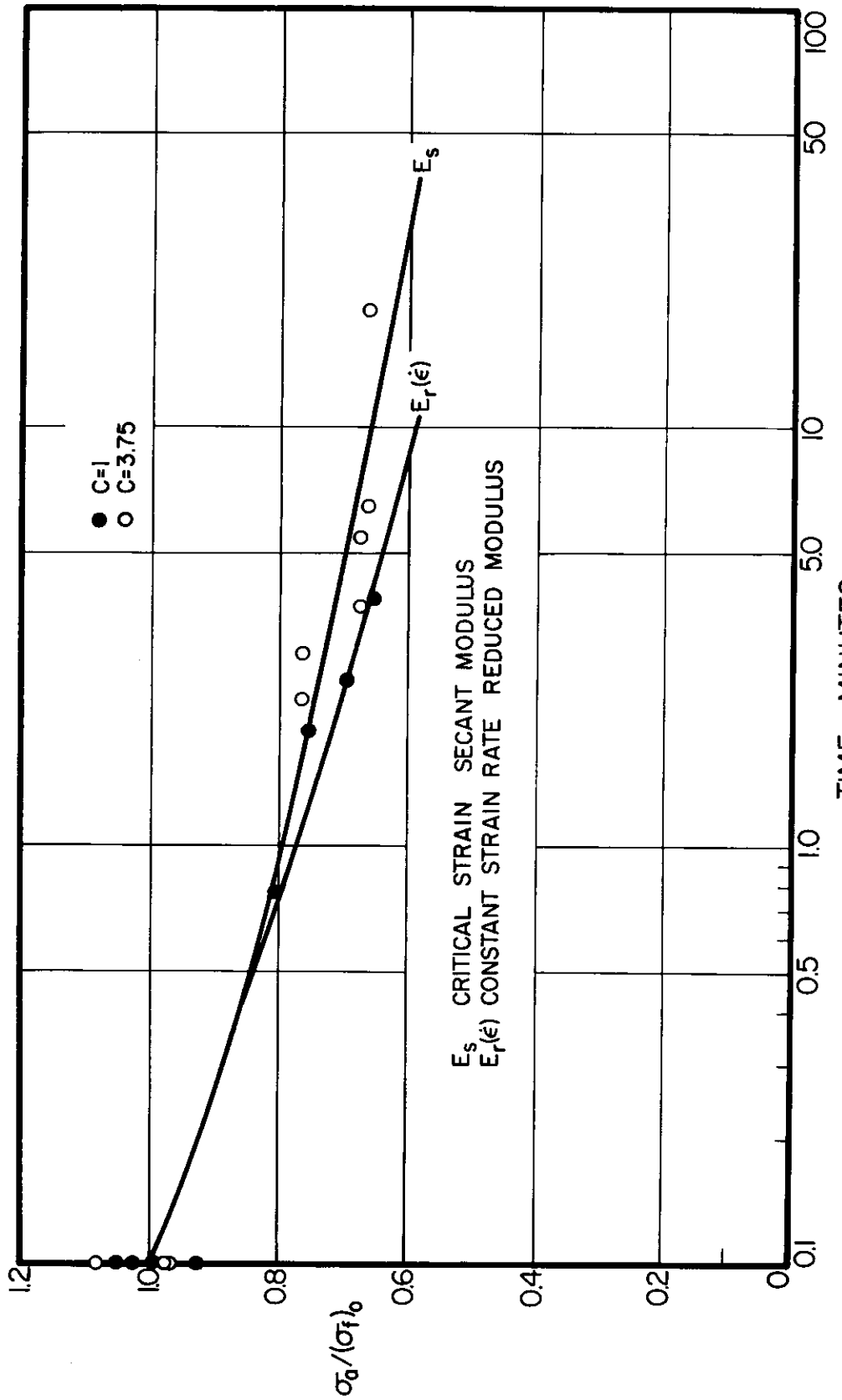

FIGURE 17 CORRELATION OF CONSTANT STRAIN RATE-REDUCED MODULUS AND SECANT MODULUS APPROACHES TO CREEP BUCKLING EXPRESSED IN NORMALIZED STRESS FORM WITH EXPERIMENTS ON ALUMINUM ALLOY 2024-0 COLUMNS, $L'/\rho = 40$, AT 500°F

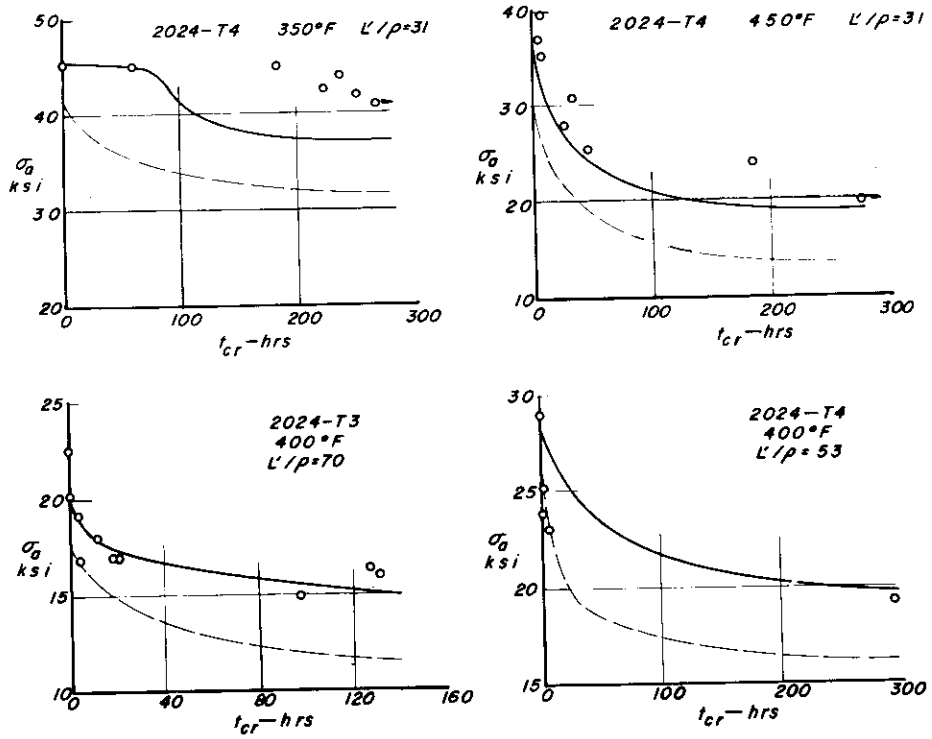

FIGURE 18 CORRELATION OF SECANT MODULUS AND ISOCHRONOUS TANGENT MODULUS APPROACHES TO CREEP BUCKLING WITH EXPERIMENTS ON ALUMINUM ALLOY COLUMNS. EXPERIMENTAL DATA FROM REFERENCE (7).

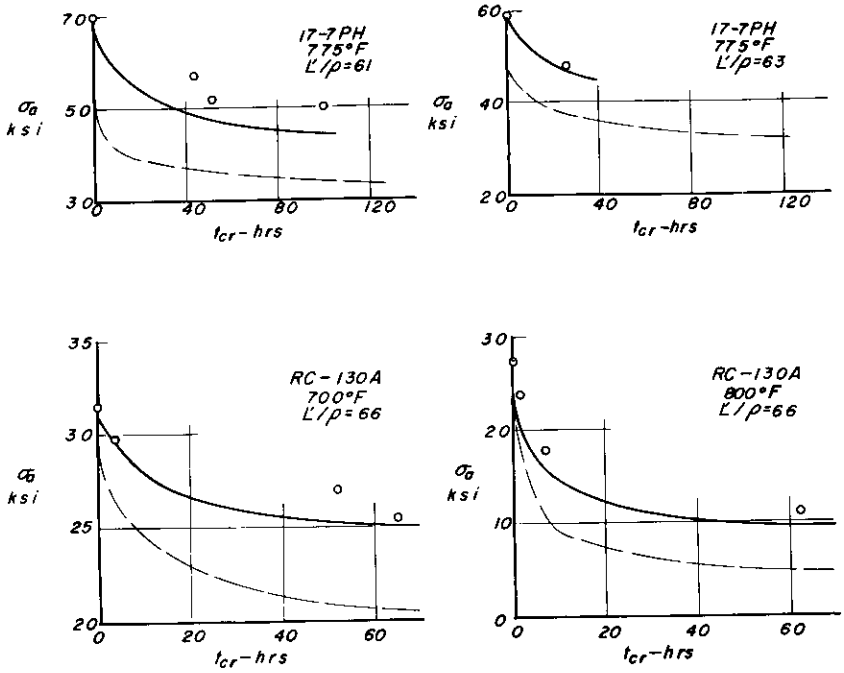

FIGURE 19 CORRELATION OF SECANT MODULUS AND ISOCHRONOUS TANGENT MODULUS APPROACHES TO CREEP BUCKLING WITH EXPERIMENTS ON STAINLESS STEEL AND TITANIUM ALLOY COLUMNS. EXPERIMENTAL DATA FROM REFERENCES (6) AND (7).

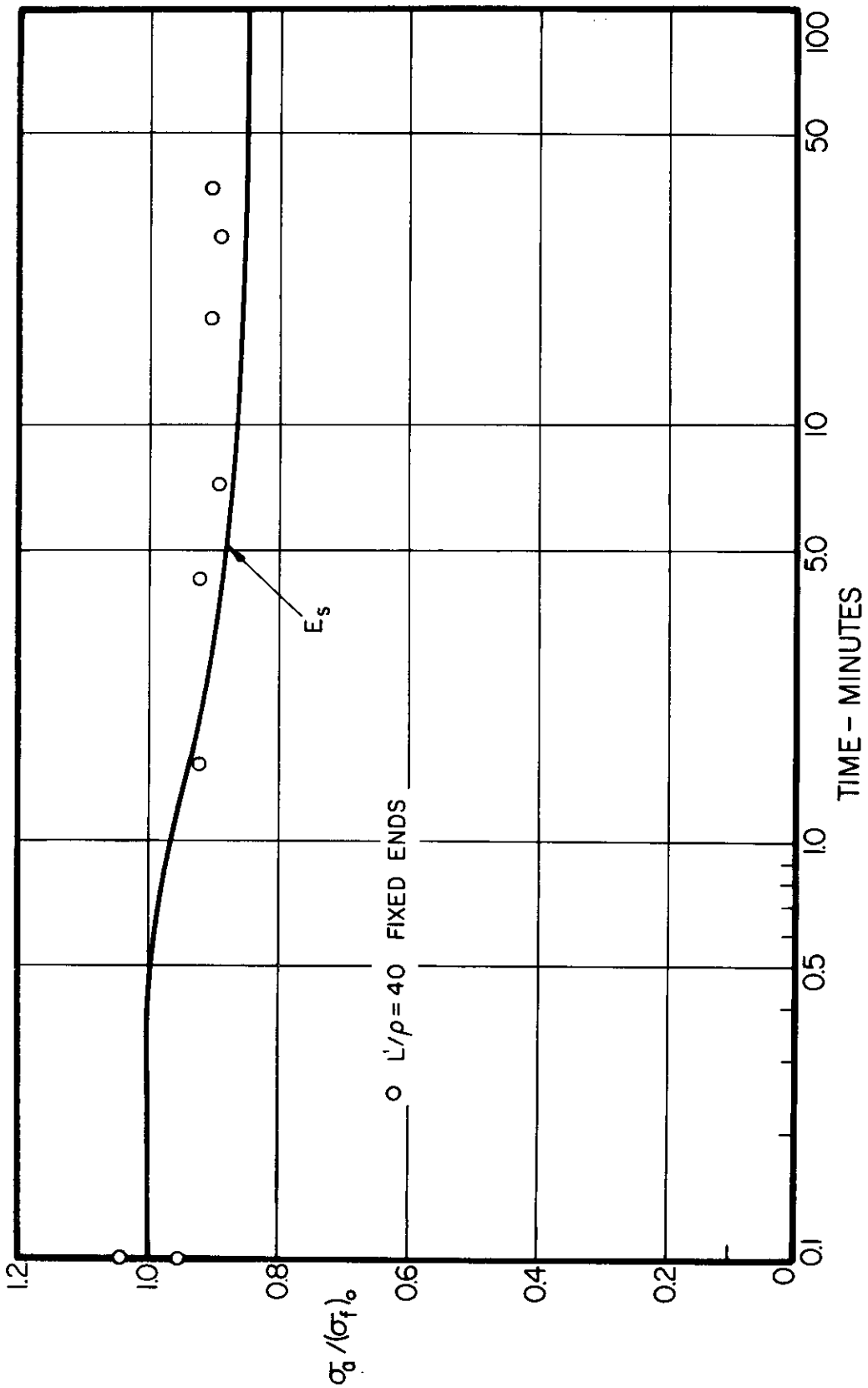

FIGURE 20 CORRELATION OF THE SECANT MODULUS APPROACH TO CREEP BUCKLING WITH EXPERIMENTS ON Ti-7Al-4Mo TITANIUM ALLOY COLUMNS AT 950°F. DATA FROM REFERENCE (9)